Energy stored during deformation of crystallizing TPU foams

Abdelmonem Lachhab, Eric Robin, Jean-Benoit Le Cam, Frédéric Mortier, Yvon Tirel, Frédéric Canevet

Energy stored during deformation of crystallizing TPU foams

A. Lachhab[1,2,3] | E. Robin[1,2] | J.-B. Le Cam[1,2] | F. Mortier[2,3] | Y. Tirel[2,3] | F. Canevet[2,3]

The hysteresis loop observed in the mechanical response of elastomers is classically assumed to be due to viscosity. In this study, a complete energy balance is carried out during cyclic deformation of compact and foamed crystallizing thermoplastic polyurethanes. Results show that viscosity is not the only phenomenon involved in the hysteresis loop formation: A significant part of the mechanical energy brought is not dissipated into heat and is stored by the material when the material changes its microstructure, typically when it is crystallizing. Some of this energy is released during unloading, when melting occurs, but with a different rate, which contributes to the hysteresis loop. The part of the mechanical energy stored by the material has been quantified through the γ_{se} ratio (Loukil et al. (2018) European Polymer Journal, 98, 448–455) to investigate the effects of the loading rate and the void volume fraction on the energetic response of thermoplastic polyurethane.

KEYWORDS

energy stored, infrared thermography, intrinsic dissipation, strain-induced crystallization, TPU foam

1 | INTRODUCTION

The thermoplastic polyurethanes (TPUs) exhibit specific properties such as chemical resistance, biocompatibility, and high elasticity and are therefore good candidates for many applications: medicine, transport, agri-food, and military industries, to name a few. From a mechanical point of view, they are subjected to many anelastic phenomena such as mechanical hysteresis, residual stretch, and softening.[1-6] These phenomena strongly depend on the material formulation.

When foamed, TPU becomes more deformable and are still dissipative.[7-10] Even though the energy dissipation capacity of TPU is classically measured as the mechanical hysteresis area, no study investigates the physical origin of this dissipation.

Different phenomena can be responsible for the mechanical hysteresis.

(a) The intrinsic dissipation (d_1), due to internal friction and/or damage, which leads to self-heating;
(b) the thermal dissipation (d_2; in nonadiabatic test conditions). If heat is exchanged with the exterior of the specimen, a hysteresis loop in the stretch–stress relationship forms, even for purely elastic materials. In most of the tests performed, the loading rate is sufficiently high and the thermal dissipation does not really contribute to the mechanical hysteresis;
(c) the part of the mechanical energy used by the material to change its microstructure $W_{structure}$. In this case, all the work done to the system is not measured as a temperature change (see, for instance, the recent study by Mott et al.[11] on

polyurea). The material stores part of the mechanical energy brought and releases it (or a part of it) with a different kinetics.[12, 13]

Such analysis is classically carried out in metallic materials, since the pioneering work by Farren and Taylor[14] and Taylor and Quinney[15] who measured the latent energy remaining after cold working in a metal under quasistatic monotonous loadings. Today, the fraction of the anelastic deformation energy rate irreversibly converted into heat is studied through the Taylor–Quinney ratio.[16-20] Polymers have then benefited from this approach to improve the understanding of the deformation processes.[21-24] Concerning elastomers, only two recent studies by Le Cam and co-workers investigate the energetic behaviour and the energy storage during deformation.[12, 13] In unfilled natural rubber, the stored energy is mainly due to strain-induced crystallization (SIC)/melting process. No irreversibilities take place, and no energy is dissipated into heat. In the case of filled uncrystallizable nitrile butadiene rubber (NBR), only a part of the mechanical energy is dissipated into heat, due to viscous effect induced by carbon black fillers.[13] Indeed, adding fillers also induces energy storage. To further discuss on the relative contribution of the energy stored in the hysteresis loop of rubbers, authors proposed a ratio γ_{se}, written in terms of energies over one mechanical cycle as follows[13]:

$$\gamma_{se} = \frac{W_{stored}^{cycle}}{W_{hyst}^{cycle}}. \tag{1}$$

W_{stored}^{cycle} is the energy stored over one cycle, and W_{hyst}^{cycle} is the energy of the hysteresis loop.

- If γ_{se} tends to be 0, no energy is stored during the deformation process. The whole hysteresis loop is due to the intrinsic dissipation, and the corresponding energy is dissipated into heat,
- If γ_{se} tends to be 1, the whole hysteresis loop corresponds to energy stored, and no intrinsic dissipation is detected. This is typically the case in unfilled natural rubber.[25]

The physical meaning of this ratio is different from the Taylor–Quinney coefficient, because it is not measured from a latent energy remaining after cold working, because the energy stored in the elastomer network can released. Estimating such a ratio is of importance to better compare material formulations, especially in relation to their fatigue resistance. In case of TPU materials, no study in this field has been reported in the literature while they are submitted to mechanical cycles in many applications. In the present work, a complete energy balance is carried out in order to determine the effects of the loading rate, the number of cycles (accommodation) and the void volume fraction on the energetic behaviour of compact and foamed TPUs. For this purpose, infrared thermography was used to determine heat sources using the heat diffusion equation. The paper is organized as follows. Section 2 recalls the thermodynamic framework. Section 3 presents the technique used to elaborate the samples, the loading conditions, and the thermal measurement during the mechanical tests. Section 4 gives the results and compares the TPUs with different densities according to their mechanical and calorimetric responses. Calorific effects of SIC are more particularly addressed. Concluding remarks close the paper.

2 | THERMODYNAMIC FRAMEWORK

Identifying the phenomena involved in the mechanical energy dissipation requires to define the different quantities needed for energy balances, especially the mechanical energy, the heat sources, and the intrinsic dissipation. They are introduced in the following.

2.1 | Total strain energy density and hysteresis loop

The strain energy density W_{strain} (in J/m^3) is the energy brought mechanically to deform the material. It corresponds to the area under the load (unload) strain–stress curve and is calculated as follows:

$$W_{strain}^{load} = \int_{load} \pi \quad d\lambda \quad \text{and} \quad W_{strain}^{unload} = \int_{unload} \pi \quad d\lambda. \tag{2}$$

λ is the stretch defined as the ratio between current and initial lengths. π is the nominal stress, defined as the force per unit of initial (undeformed) surface. If the material's behaviour is purely elastic and if the test is carried out under adiabatic loading conditions, the mechanical response obtained during a load–unload cycle is such that no hysteresis loop

forms ($W_{strain}^{load} = W_{strain}^{unload}$). If a hysteresis loop forms, the mechanical energy dissipated over one cycle W_{hyst}^{cycle} is defined as follows:

$$W_{hyst}^{cycle} = W_{strain}^{load} - W_{strain}^{unload}. \tag{3}$$

From this energy, a quantity P_{hyst}^{cycle} is calculated in W/m^3. It is obtained by dividing W_{hyst}^{cycle} by the cycle duration. It is therefore an energy density per time unit or an energy rate.

2.2 | Heat sources

During the mechanical cycle, the material produces and absorbs heat. Under nonadiabatic conditions, corresponding temperature variations are influenced by heat diffusion effects. To account for these effects, a simplified formulation of the heat diffusion equation is used (see Chrysochoos and Louche[26] for further details), considering the heat power density field as homogeneous during uniaxial tensile loading:

$$\rho C \quad \left(\dot{\theta} + \frac{\theta}{\tau}\right) = s, \tag{4}$$

where ρ is the initial density, C is the specific heat, θ is the temperature variation, and τ is a characteristic time that is identified from a natural return to ambient temperature. The right-hand side of Equation 4 corresponds to the heat sources. It can be divided into two terms that differ in nature:

- the intrinsic dissipation d_1: This positive quantity corresponds to the heat production due to mechanical irreversibilities during the deformation process, for instance viscosity or damage;
- the thermomechanical couplings s_{tmc}: They correspond to the couplings between the temperature and the other state variables and describe reversible deformation processes. Consequently, their integration with respect to time over one cycle is null.

Therefore, the temporal integration of Equation 4 over one mechanical cycle provides the energy density due to intrinsic dissipation $W_{intrinsic}^{cycle}$:

$$W_{intrinsic}^{cycle} = \int_{cycle} (s_{tmc} + d_1) \quad dt = \int_{cycle} d_1 \quad dt. \tag{5}$$

$W_{intrinsic}^{cycle}$ is divided by the cycle duration to obtain the energy rate P_{d_1} due to intrinsic dissipation or the average intrinsic dissipation over one cycle. It should be noted that d_1 is possibly nonconstant during the mechanical cycle.

2.3 | Energy balance

The energy balance consists in comparing the energy contained in the mechanical hysteresis (W_{hyst}^{cycle}), more precisely P_{hyst}^{cycle}, with P_{d_1}. Using the energy rate instead of the energy itself enables us to compare the energetic response from one cycle to another one. If both quantities are equal for a given cycle, all the mechanical energy of the hysteresis loop is converted into heat. Else, it is necessary to distinguish the part of the mechanical energy converted into heat from the one stored by the material to change its microstructure. For that purpose, the ratio γ_{se} recently proposed by Le Cam and co-workers[13] is used:

$$\gamma_{se} = \frac{W_{stored}^{cycle}}{W_{hyst}^{cycle}}, \tag{6}$$

where $W_{stored}^{cycle} = W_{hyst}^{cycle} - W_{intrinsic}^{cycle}$.

The subsequent question is whether all (or a part of) the energy stored is released or not during unloading. For crystallizable unfilled natural rubber, it has been shown that all the energy stored is released, but with a different rate, which forms a hysteresis loop. At the end of the mechanical cycle, the material returns to the same thermal and deformation states (see more details in Chrysochoos et al.[27]). This will be discussed for the case of the TPU studied in the following.

3 | EXPERIMENTS

3.1 | Materials and experimental setup

The material considered here is a TPU referred to as Irogran A87H4615 TPU marketed by the Huntsman corporation (The Woodlands, Texas). It is elaborated by reacting together a diisocyanate, a macrodiol (long chain diol), which is a polyester, and a small molecule chain-extender (butane diol).[28] This TPU has a melting temperature of 180 °C, a density equal to 1.20 kg/dm^3, and a hardness of 85 Shore A at 23 °C. The TPU is mixed with carbon dioxide in its supercritical state during injection, in order to form cells and to significantly decrease its density. The forming process is based on two patents[29, 30] and is more precisely described in Primel et al. [28] and Lachhab et al.[3] The samples were obtained by cutting a bar with a water jet cutting device. Three densities were compared: 1.2, 0.7, and 0.5 kg/dm^3, the corresponding samples are denoted, respectively, $d_{1.2}$, $d_{0.7}$, and $d_{0.5}$ in the following. The density equal to 1.2 corresponds to the compact form, obtained without mixing the TPU with carbon dioxide. The sample geometry is presented in Figure 1.

It can be noted that this geometry prevents the sample from any sliding in the grips. Figure 2 presents micrographs of the cellular microstructure of specimens $d_{0.7}$ and $d_{0.5}$ in the vicinity of the specimen surface. A skin effect is observed close to the surface. The skin contains a very few number of cells. It is therefore stiffer than the rest of the sample and could influence significantly the mechanical response of the foamed samples. Its thickness is about 1 mm for both densities. This is the reason why the skin formed during the moulding was removed from the bar by using water jet cutting.

3.2 | Loading conditions

Uniaxial tensile loadings were carried out with a 5543 Instron testing machine. Tests were performed under prescribed displacement. The signal shape was triangular to ensure a constant strain rate during loading and unloading. As shown in Figure 1, mechanical tests were performed by applying five mechanical cycles at four increasing maximum stretch levels ($\lambda_1 = 1.5$, $\lambda_2 = 2$, $\lambda_3 = 2.5$, $\lambda_4 = 3$). The number of cycles at a given stretch was chosen to ensure the mechanical response to stabilize, in order to investigate softening effects. Two loading rates were applied, ±100 and ±300 mm/min.

3.3 | Thermal measurement

Temperature field measurements were performed using an FLIR X6540sc InSb infrared camera (640 × 512 pixels, wavelength ranges between 1.5 and 5.1 μm, detector pitch of 15 μm), with an integration time equal to 1,000 μs. The acquisition frequency was set at 50 Hz. The thermal resolution, namely, the noise-equivalent temperature difference, was equal to 20 mK at 25 °C. The calibration of the camera detectors was performed with a black body using a Non-Uniformity Correction procedure. Temperature measurement was performed at the specimen centre, by averaging the temperature in a small zone of 5 × 5 pixels at the centre of the sample. Temperature variation was obtained by subtracting the initial averaged temperature to the current one. As the zone moves during the test, a suitable movement compensation technique enabled us to track this zone during the test (see Pottier et al.,[31] Toussaint et al.,[32]or Samaca Martinez et al.[33] for further information on this technique). To process IR images, emissivity of the polyurethane surface was set at 0.9 for compact TPU and 0.62 for TPU foams.

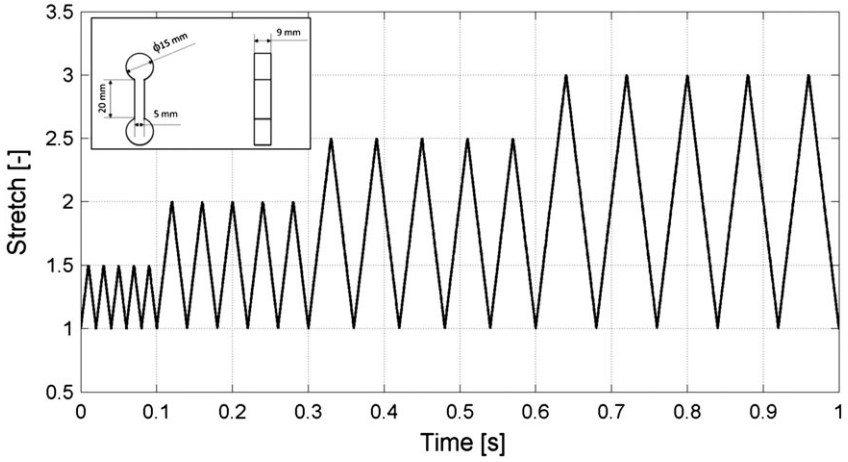

FIGURE 1 Sample geometry and loading conditions

4 | RESULTS AND DISCUSSION

4.1 | Mechanical responses

The mechanical responses obtained are presented for samples $d_{1.2}$, $d_{0.7}$, and $d_{0.5}$ at ±100 and ±300 mm/min in Figure 3(a) and 3(b), respectively.

These figures give the nominal stress, defined as the force per initial surface ratio, in relation to the stretch. For each loading condition and density, typical effects in the mechanical response of elastomers are observed: softening, residual stretch, and hysteresis. These effects have been widely investigated in the literature.[2, 5, 6, 34] Concerning more particularly the present TPU, an exhaustive analysis is provided in Lachhab et al.[3] and is therefore not precisely detailed here. The main results can be summed up as follows:

- decreasing the density leads to a decrease in the global stiffness and in the hysteresis area, slightly increases the residual stretch, and does not affect significantly the stress softening;
- the loading rate has no significant influence on the stress softening, although it influences more the residual stretch and the hysteresis area. It should be noted that the loading rate does not affect significantly the stiffness, which is a less intuitive result.

These mechanical curves are used to determine the strain energy densities needed for energy balances.

4.2 | Calorimetric responses

Temperature measurements have been performed during the mechanical tests. Parameter τ have been characterized for each test configuration and material tested, and the corresponding heat sources have been determined (see Equation 4). It should be noted that, in practice, τ is usually identified from a natural return of the specimen to room temperature after a heating. As it was shown in Samaca Martinez et al.,[25, 35] τ strongly depends on the stretch. The identification of τ was therefore performed for the different densities and stretch levels applied.

Results obtained are presented in Figure 4(a) and 4(b) for the three densities tested at ±100 and ±300 mm/min, respectively.

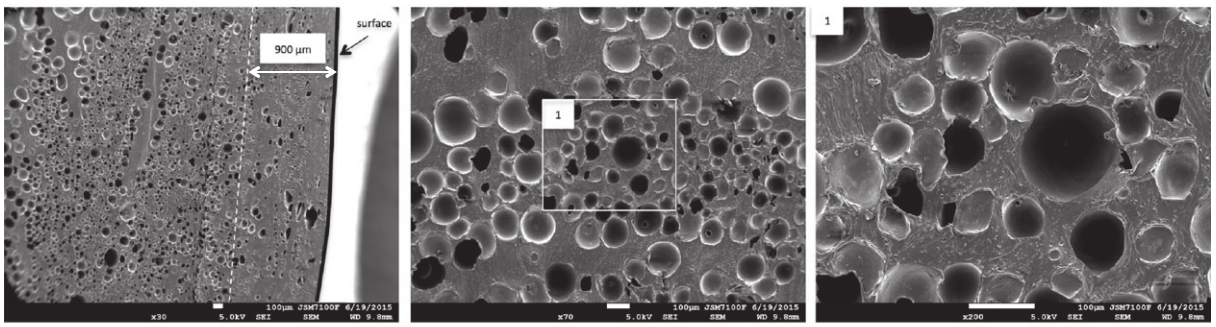

(a) $d_{0.7}$

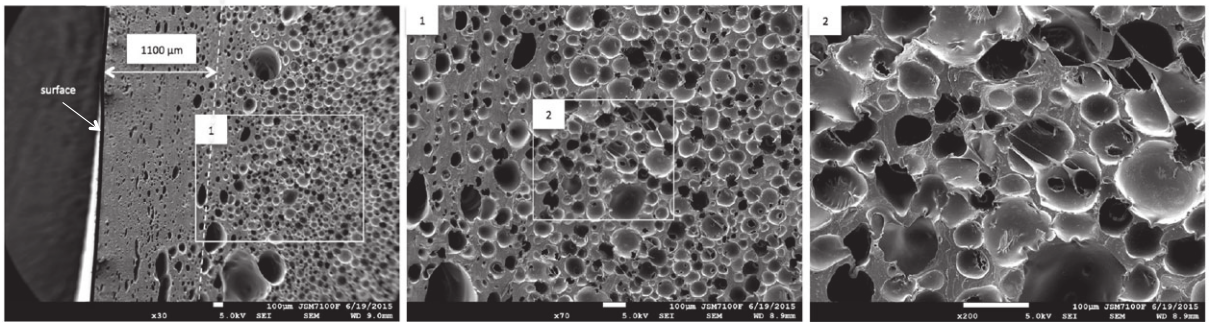

(b) $d_{0.5}$

FIGURE 2 SEM micrographs of the skin

As shown in these figures, the heat power density increases when the TPU is stretched and decreases when the stress is released. The effect of the entropic coupling is therefore the most significant. The higher the density, the higher the maximum heat sources produced. As highlighted by the mechanical responses, the material accommodates each time the maximum stretch is increased, which explains that the highest value of the heat sources is reached for the first mechanical cycles of each set.

Let us now consider the calorimetric response versus the stretch for the three densities at the two loading rates (Figures 5 and 6). In this analysis, the calorific response of the compact TPU $d_{1.2}$ at ±300 mm/min (Figure 5a) is chosen as the reference one. For the first two sets of stretches applied ($\lambda = 1.5$ and $\lambda = 2$), heat power densities are symmetrical with respect to the abscissa axis, meaning that the elastic coupling is the preponderant contribution to the calorific response. Therefore, no significant intrinsic dissipation is produced as the curves are not shifted towards the positive heat power densities. For sets at a maximum stretch superior to 2, a strong change in the curve slope is observed during the loading (at about $\lambda = 2.1$ for the third set at $\lambda = 2.5$). As the mechanical response does not exhibit such a singularity, this cannot be due to the effect of the entropic coupling. This strong increase in the heat production is analogue to what is observed in NR when crystallizes[12, 25] and highlights that the present TPU is crystallizing under strain. The higher the maximum stretch applied, the higher the stretch at which the strong increase in the heat production is observed, and the higher the residual stretch. This means that SIC in TPU, more precisely the beginning of SIC, should be mainly driven by the stretch. For the last set of maximum stretch applied ($\lambda_4 = 3$), the maximum value of the heat sources reached is not higher than the previous sets, meaning that a saturation effect as observed in natural rubber (or a crystallinity rate decrease) could be obtained in TPU. During unloading, a strong dissymmetry, comparable to what is obtained in NR, is observed. In the case of NR, X-ray diffraction (crystallinity versus stretch curves) shows that crystallinity is higher during unloading than during loading[36, 37] and that the dissolution of the crystalline order in NR is faster than its establishment after a strain step.[38] This demonstrates that crystallization continues during unloading in NR and this is probably what occurs in the case of the present TPU. During unloading, a strong heat absorption is observed at a stretch inferior to that at which SIC starts. This is once again analogue to NR. The next paragraph details the effect of the density and the loading rate separately.

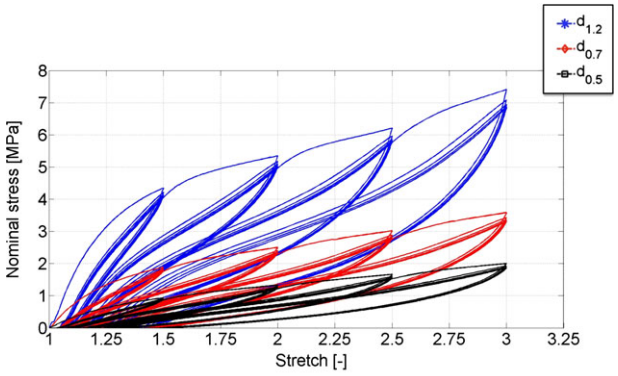

(a) $\pm 100\ mm/min$

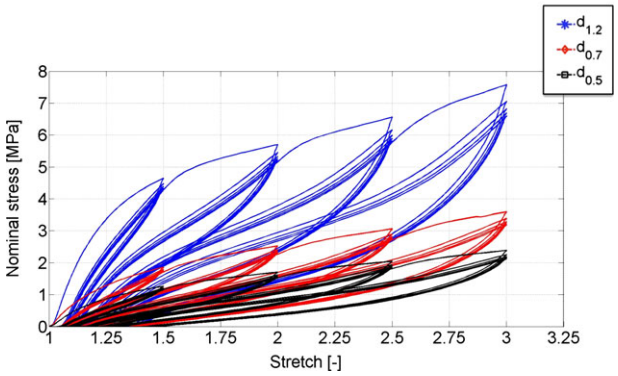

(b) $\pm 300\ mm/min$

FIGURE 3 Mechanical responses (stress vs. stretch) for the three densities

4.2.1 | Effect of the density

Let us consider the foamed TPUs at ±300 mm/min (Figure 5b and 5c). For $d_{0.7}$, the previous observations apply, except that the high heat production due to SIC is lower. This seems to indicate that the crystallinity is lower. For the first set of mechanical cycles, SIC starts at a stretch of about 1.4 for $\lambda_1 = 2$, which increases for sets at higher maximum stretches, as the residual stretch also increases (SIC being driven by the strain). The fact that the stretch at which SIC starts is lower

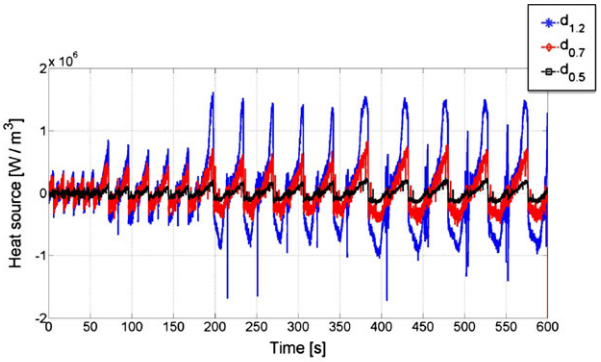

(a) $\pm 100\ mm/min$

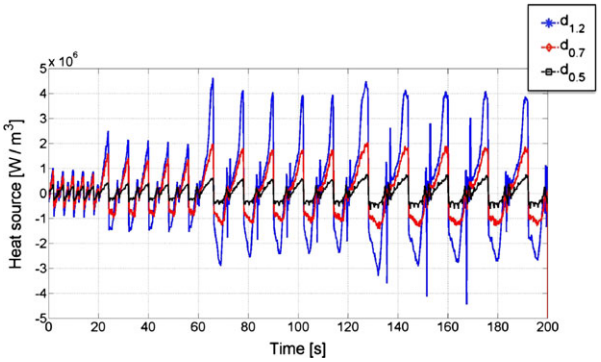

(b) $\pm 300\ mm/min$

FIGURE 4 Heat sources versus time for the different densities at the two loading rates

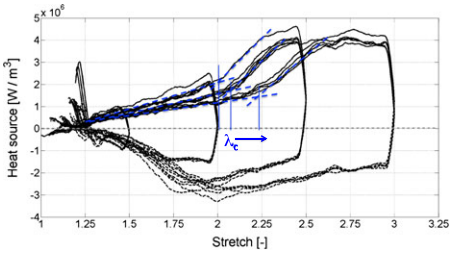

(a) $d_{1.2}$

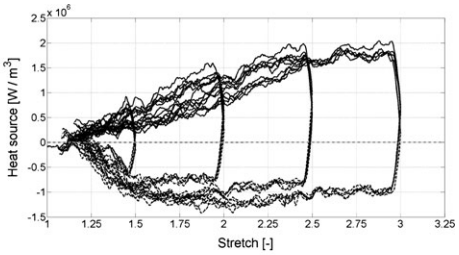

(b) $d_{0.7}$

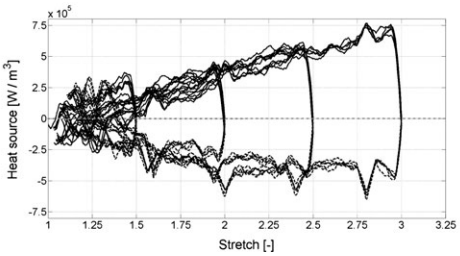

(c) $d_{0.5}$

FIGURE 5 Heat sources versus stretch for the different densities at ±300 mm/min

in the foamed is explained by the fact that the cavity wholes concentrate the strain. Nevertheless, the macromolecular mobility is decreased, which decreases the ability of the macromolecule network to form crystallites and explains why the heat production is lower than in compact TPU. These reasons explain why for $d_{0.5}$, it was not possible to detect SIC with the technique used. Increasing the void volume fraction is in a strong analogy with the addition of fillers in crystallizable rubbers in terms of effects on crystallinity. Note that it induces the reverse effect on the stiffness.

4.2.2 | Effect of the loading rate

Heat sources increase with the loading rate, which is due to the couplings between temperature and stretch and to intrinsic dissipation if any. When the loading rate is increased by a factor 3, the heat sources also. As the mechanical response is quite the same between the two loading rates, this means that the heat sources are mainly due to the coupling between temperature and stretch, in other terms the intrinsic dissipation is very low. Nevertheless, a hysteresis loop is observed in the mechanical response, which means that the material uses a part of the mechanical energy to change its microstructure. This will be discussed in the next paragraph. Moreover, conclusions drawn on the effect of the density on the calorific response are not changed by decreasing the loading rate.

4.2.3 | Energy balance

To further discuss on the energetic behaviour and especially on physical origin of the mechanical hysteresis, P_{hyst}^{cycle} and P_{d_1} over each cycle are plotted in the same diagram in relation to the density and for the two loading rates (Figures 7 and 8). In the case where the mechanical hysteresis is due to viscosity only, P_{hyst}^{cycle} and P_{d_1} are equal, that is, all the energy contained in the hysteresis loop is converted into heat. If P_{d_1} is inferior to P_{hyst}^{cycle}, the material uses a part of the mechanical energy to change its microstructure. In other words, the material stores energy. In Figures 7 and 8, the green zones stand for the energy density per time unit due to microstructure changes (P_{stored}^{cycle}), the red zones for P_{d_1}. Figure 7, giving results for the lowest loading rate, shows that P_{d_1} is not the main contribution to P_{hyst}^{cycle}, whatever the density and the stretch considered. Thus, the material uses part of the energy brought mechanically to change its microstructure. The main physical origin involved in the hysteresis loop is therefore not viscosity in the range of the loading rates applied. This is in the same line as results recently obtained by Mott et al.[11] who have shown that during extension, the polyurea they tested uses a significant part of the mechanical energy to change its microstructure, whatever the stretch level considered. This is analogue with what was observed in NR by Le Cam.[12] P_{hyst}^{cycle} increases with the stretch level and the density. Furthermore, the higher value of P_{hyst}^{cycle} is reached at each first cycle, and we consider that it is stabilized from the second cycle of each set of maximum stretch. This has to be put into perspective with the strong residual stretch observed at the first cycles.

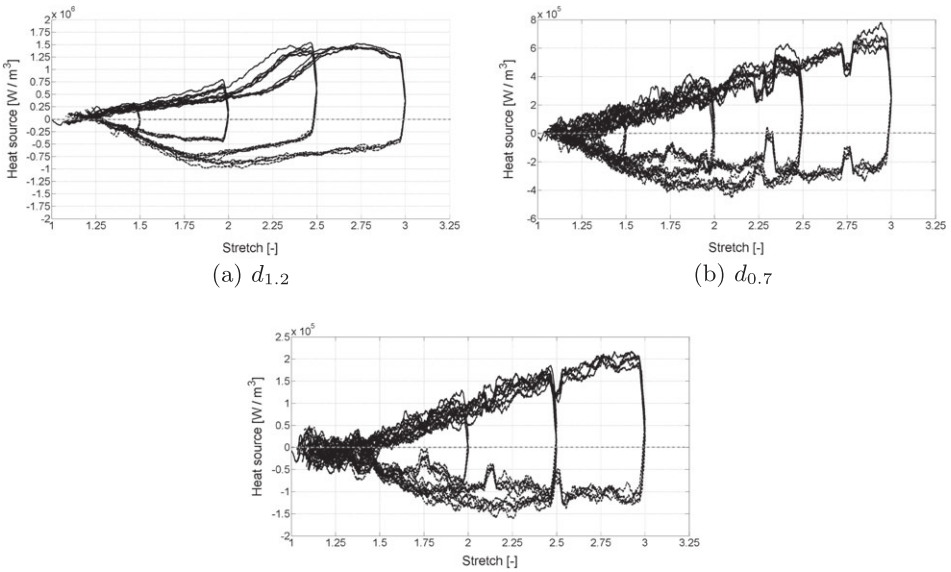

(a) $d_{1.2}$ (b) $d_{0.7}$

(c) $d_{0.5}$

FIGURE 6 Heat sources versus stretch for the different densities at ±100 mm/min

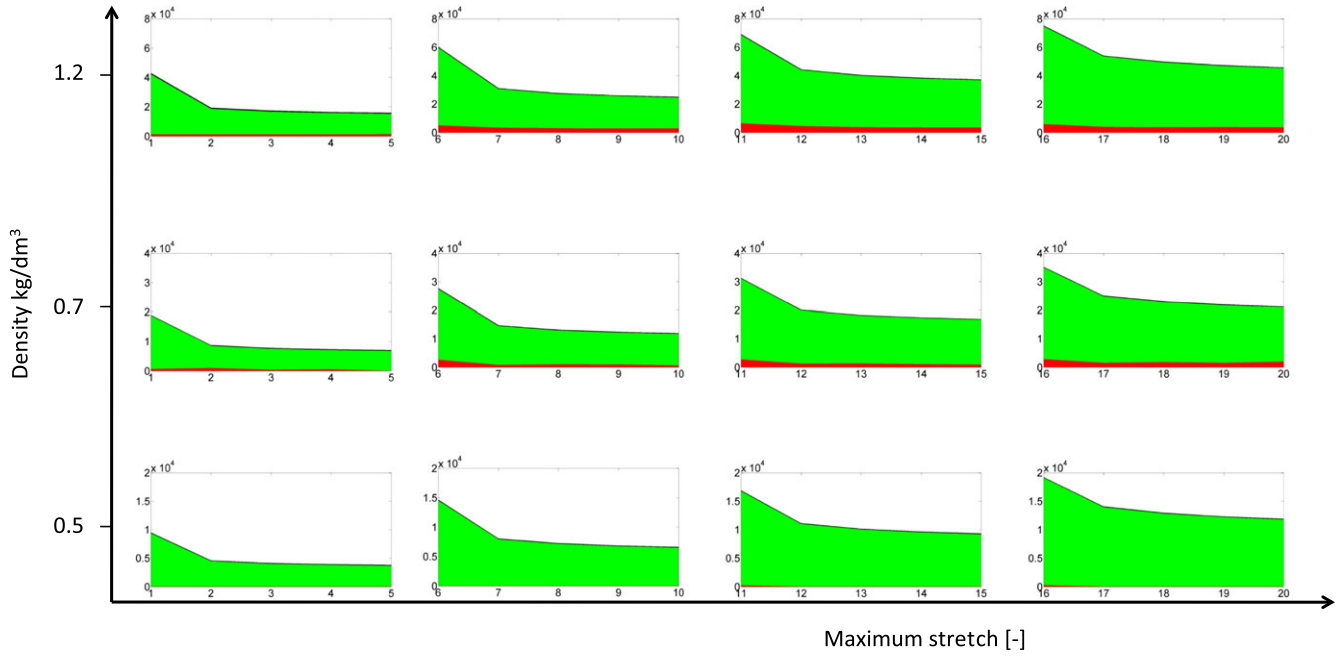

FIGURE 7 Maps of the strain power density and intrinsic dissipation over each cycle in relation to the density and the stretch (±100 mm/min)

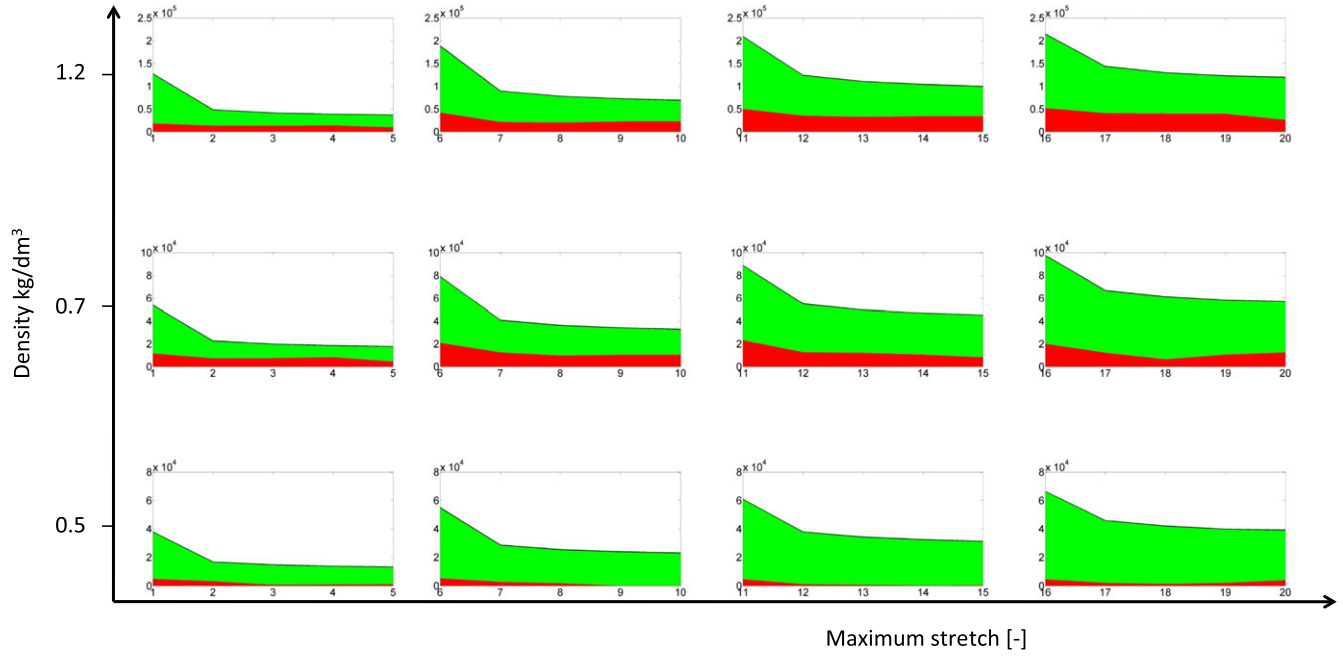

FIGURE 8 Maps of the strain power density and intrinsic dissipation over each cycle in relation to the density and the stretch (±300 mm/min)

This is not observed the next cycles (no increase in the residual stretch, no decrease in the value of P_{hyst}^{cycle}). As P_{d_1} is very low whatever the cycles considered, this might mean that some latent heat remains in the material after the first cycles, in other words, all the crystallites do not melt. This assumption has to be verified by further X-ray diffraction experiments.* These results are then compared with those obtained at the highest loading rate (see Figure 8). For samples $d_{1.2}$ and $d_{0.7}$,

*It should be noted that if all the crystallites formed do not melt, all the heat produced during crystallization is not reabsorbed during melting, meaning that an additional apparent P_{d_1} can be detected

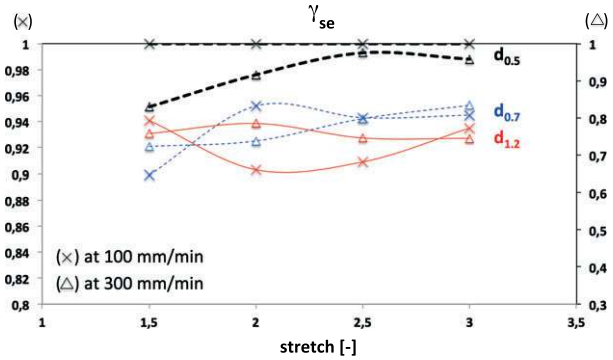

FIGURE 9 γ_{se} for the three densities at ±100 mm/min (primary axis on the left) and ±300 mm/min (secondary axis on the right)

the viscous effects are found to increase with the loading rate, the density, and the maximum stretch applied. The increase of the viscous effect, that is, the decrease in the energy stored, has already been highlighted in other polymer materials such as PA66.[39] This is not observed for sample $d_{0.5}$ for which P_{d_1} remains low. This is a remarkable result that was previously observed in Lachhab et al[3] by considering the thermal response. Indeed, for this density level, no self-heating was observed, even when the loading rate was increased by a factor 3. Such a result is of importance for designing TPU parts submitted to cyclic loadings. In order to summarize these results, the ratio γ_{se} has been calculated for every second cycles, for which the mechanical stabilization is obtained. This leads to the diagram in Figure 9, given γ_{se} in relation to the density, the loading rate, and the stretch. It should be noted that the calorific response is not stabilized from the second cycle, especially for results obtained samples $d_{0.5}$ at ±300 mm/min. In this case, P_{d_1} tends to zero, which means that γ_{se} would be close to 1 whatever the stretch applied, similarly to what is observed at ±100 mm/min.

Such a representation opens a new way to investigate the thermomechanical and energetic behaviour of elastomers. Further investigations are currently carried out in our laboratory to investigate the physical meaning of the values of γ_{se} in relation to the material microstructure and the experimental parameters.

5 | CONCLUSION

The present study investigates the thermomechanical and calorific behaviour of TPU foams. Complete energy balances have been carried out in order to highlight the physical origin of the hysteresis loop. Different densities were tested, including the compact state, which ensures a relevant characterization of the effect of the cell volume fraction on the TPU's formulation used. A series of cyclic uniaxial tensile tests were carried out at different loading rates and different sample densities. The softening was found to be only dependent on the maximum stretch applied. Contrarily, the residual stretch and the hysteresis are clearly affected by changes in the loading rate and the density (the amount of viscous matter available). The calorimetric response has shown that the material's elasticity is mainly entropic, but it uses mechanical energy brought to it to change its microstructure. This is in good agreement with measurements recently performed in a compact polyurea in Mott et al.[11] For samples of the highest density, viscous effects are found to increase with the loading rate, the density, and the maximum stretch applied. This is not observed for sample of the lowest density, for which the intrinsic dissipation remains low. Therefore, for the lowest density, no self-heating was observed, even when the loading rate was increased by a factor 3. To fully address viscoelastic effects, complementary experiments at loading rates of one order of magnitude higher are currently carried out. Furthermore, the fact that the material is able to store part of the mechanical energy is in a strong analogy with what is observed in natural rubber. This probably explains why both materials are among the most resistant to the crack growth. Such a result is of importance when designing foamed TPU parts submitted to cyclic loadings.

ACKNOWLEDGEMENTS

The authors thank the Cooper Standard France company for supporting this work and for fruitful discussions. The authors thank also the National Center for Scientific Research (MRCT-CNRS and MI-CNRS) and Rennes Metropole for supporting this work financially.

ORCID

J.-B. Le Cam http://orcid.org/0000-0002-2366-2512

REFERENCES

[1] L. Bartolome, J. Aurrekoetxea, M. A. Urchegui, W. Tato. *Mater. Des.* **2013**, *49*, 974.

[2] D. Blundell, G. Eeckhaut, W. Fuller, A. Mahendrasingam, C. Martin. *Polymer* **2002**, *43*, 5197.

[3] A. Lachhab, E. Robin, J.-B. Le Cam, F. Mortier, Y. Tirel, F. Canevet. *Polymer* **2017**, *126*, 19.

[4] H. Qi, M. Boyce. *Mech. Mater.* **2005**, *37*, 817.

[5] E. Unsal, B. Yalcin, I. Yilgor, E. Yilgor, M. Cakmak. *Polymer* **2009**, *50*, 4644.

[6] F. Yeh, B. Hsiao, B. Sauer, S. Michael, H. Siesler. *Macromolecules* **2003**, 1940.

[7] M. F. Alzoubi, E. Y. Tanbour, R. Al-Waked, Compression and Hysteresis Curves of Nonlinear Polyurethane Foams Under Different Densities, in Strain Rates and Different Environmental Conditions, **2011**, ASME International Mechanical Engineering Congress and Exposition, Denver, Colorado, USA, 101–109.

[8] P. J. Blatz, W. L. Ko. *Trans. Soc. Rheol.* **1962**, *6*, 223.

[9] F. Saint-Michel, L. Chazeau, J.-Y. Cavaillé, E. Chabert. *Compos. Sci. Technol.* **2006**, *66*, 2700.

[10] L. Ugarte, A. Saralegi, R. Fernandez, L. Martin, M. A. Corcuera, A. Eceiza. *Ind. Crops Prod.* **2014**, *62*, 545.

[11] P. Mott, C. Giller, D. Fragiadakis, D. Rosenberg, C. Roland. *Polymer* **2016**, *105*, 227.

[12] J. B. Le Cam. *Polymer* **2017**, *127*, 166.

[13] M. Loukil, G. Corvec, E. Robin, M. Miroir, J.-B. Le Cam, P. Garnier. *Eur. Polym. J.* **2018**, *98*, 448.

[14] W. S. Farren, G. I. Taylor. *Proc. R. Soc. London, Ser. Math. Phys. Eng. Sci.* **1925**, *107*, 422.

[15] G. I. Taylor, H. Quinney. *Proc. R. Soc. London Math. Phys. Eng. Sci.* **1934**, *143*, 307.

[16] A. Chrysochoos. *J. de Mec. Theorique et Appliquee* **1985**, *5*, 589.

[17] A. Chrysochoos, O. Maisonneuve, G. Martin, H. Caumon, J. O. Chezeau. *Nucl. Eng. Des.* **1989**, *114*, 323.

[18] J. Mason, A. Rosakis, G. Ravichandran. *Mech. Mater.* **1994**, *17*, 135.

[19] W. Oliferuk, M. Maj, B. Raniecki. *Mater. Sci. Eng., A* **2004**, *374*, 77.

[20] D. Rittel. *Mech. Mater.* **1999**, *31*, 131.

[21] A. Benaarbia, A. Chrysochoos, G. Robert. *Polym. Test.* **2014**, *34*, 155.

[22] A. Benaarbia, A. Chrysochoos, G. Robert. *Polym. Test.* **2015a**, *41*, 92.

[23] D. Rittel. *Mech. Mater.* **2000**, *32*, 131.

[24] D. Rittel, Y. Rabin. *Mech. Mater.* **2000**, *32*, 149.

[25] J. R. Samaca Martinez, J.-B. Le Cam, X. Balandraud, E. Toussaint, J. Caillard. *Polymer* **2013b**, *54*, 2727.

[26] A. Chrysochoos, H. Louche. *Int. J. Eng. Sci.* **2000**, *38*, 1759.

[27] A. Chrysochoos, V. Huon, F. Jourdan, J. Muracciole, R. Peyroux, B. Wattrisse. *Strain* **2010**, *46*, 117.

[28] A. Primel, J. Ferec, G. Ausias, Y. Tirel, J.-M. Veille, Y. Grohens. *J. Supercrit. Fluids* **2017**, *122*, 52.

[29] J. Colton, N. Suh, Microcellular foams of semi-crystaline polymeric materials, US Patent 5160674, **1992**.

[30] J. Martini-Vvedensky, N. Suh, F. Waldman **1984**.

[31] T. Pottier, M.-P. Moutrille, J.-B. Le Cam, X. Balandraud, M. Grédiac. *Exp. Mech.* **2009**, *49*, 561.

[32] E. Toussaint, X. Balandraud, J.-B. L. Cam, M. Grediac. *Polym. Test.* **2012**, *31*, 916.

[33] J. R. Samaca Martinez, J.-B. Le Cam, X. Balandraud, E. Toussaint, J. Caillard. *Polymer* **2013a**, *54*, 2717.

[34] B. Grady, S. Cooper, *in The science and technology of rubber*, (Eds: JE Mark, B Erman), Elsevier Inc, San Diego **2005**.

[35] J. R. Samaca Martinez, J.-B. Le Cam, X. Balandraud, E. Toussaint, J. Caillard. *Eur. Polym. J.* **2014**, *55*, 98.

[36] B. Huneau. *Rubber Chem. Technol.* **2011**, *84*, 425.

[37] N. Yijing, G. Zhouzhou, W. Ya, H. Tongfan, Z. Zhiping. *Polym. J.* **2017**, *49*, 309.

[38] K. Bruening, K. Schneider, S. V. Roth, G. Heinrich. *Macromolecules* **2012**, *45*, 7914.

[39] A. Benaarbia, A. Chrysochoos, G. Robert. *Polym. Test.* **2015b**, *41*, 92.